Global Change Biology

Global Change Biology (2013) **19**, 3516–3528, doi: 10.1111/gcb.12313

A large proportion of North American net ecosystem production is offset by emissions from harvested products, river/stream evasion, and biomass burning

DAVID P. TURNER*, ANDREW R. JACOBSON†, WILLIAM D. RITTS*, WEILE L. WANG‡ and RAMAKRISHNA NEMANI‡

Department of Forest Ecosystems and Society, Oregon State University, Corvallis, OR 97331, USA, †University of Colorado and NOAA Earth System Research Laboratory, Boulder, CO 80305, USA, ‡NASA Ames Research Center, Moffett Field, CA 94035, USA

Abstract

Diagnostic carbon cycle models produce estimates of net ecosystem production (NEP, the balance of net primary production and heterotrophic respiration) by integrating information from (i) satellite-based observations of land surface vegetation characteristics; (ii) distributed meteorological data; and (iii) eddy covariance flux tower observations of net ecosystem exchange (NEE) (used in model parameterization). However, a full bottom-up accounting of NEE (the vertical carbon flux) that is suitable for integration with atmosphere-based inversion modeling also includes emissions from decomposition/respiration of harvested forest and agricultural products, CO_2 evasion from streams and rivers, and biomass burning. Here, we produce a daily time step NEE for North America for the year 2004 that includes NEP as well as the additional emissions. This NEE product was run in the forward mode through the CarbonTracker inversion setup to evaluate its consistency with CO_2 concentration observations. The year 2004 was climatologically favorable for NEP over North America and the continental total was estimated at 1730 ± 370 TgC yr^{-1} (a carbon sink). Harvested product emissions (316 ± 80 TgC yr^{-1}), river/stream evasion (158 ± 50 TgC yr^{-1}), and fire emissions (142 ± 45 TgC yr^{-1}) counteracted a large proportion (35%) of the NEP sink. Geographic areas with strong carbon sinks included Midwest US croplands, and forested regions of the Northeast, Southeast, and Pacific Northwest. The forward mode run with CarbonTracker produced good agreement between observed and simulated wintertime CO_2 concentrations aggregated over eight measurement sites around North America, but overestimates of summertime concentrations that suggested an underestimation of summertime carbon uptake. As terrestrial NEP is the dominant offset to fossil fuel emission over North America, a good understanding of its spatial and temporal variation – as well as the fate of the carbon it sequesters — is needed for a comprehensive view of the carbon cycle.

Keywords: atmospheric inversion model, biomass burning, carbon flux, net ecosystem exchange, net ecosystem production, river evasion

Received 17 April 2013 and accepted 29 May 2013

Introduction

Despite strong interest in quantifying North American terrestrial carbon flux in relation to its capacity to offset fossil fuel emissions, there remains considerable uncertainty about its magnitude (Gourdji *et al.*, 2012; King *et al.*, 2012). Net ecosystem exchange (NEE) of carbon dioxide has been estimated at the regional to continental scale based on 'bottom-up' approaches that rely on inventory studies or spatially distributed ecosystem process models (Hayes *et al.*, 2012; Huntzinger *et al.*, 2012). Alternatively, 'top-down' approaches are applied based on inversions built around atmospheric transport models and observations of atmospheric CO_2 concentration (Ciais *et al.*, 2010). Recently, there has been a great deal of emphasis on flux intercomparison studies that juxtapose results from different scaling approaches (Deng & Chen, 2011; Gourdji *et al.*, 2012; Schuh *et al.*, 2013). However, there are also possibilities for integrating these approaches.

The transport model used in an inversion can potentially be run in the direct 'forward' mode to evaluate the realism of bottom-up fluxes. In a forward mode simulation, atmospheric CO_2 distributions resulting from modeled fluxes are compared with available observations. In this configuration, surface fluxes are left unmodified by the estimation scheme of the inverse model. The sign and magnitude of the observation residual errors then give an indication of potential error

Correspondence: David P. Turner, tel. +541 737 5043, fax +541 737 1393, e-mail: david.turner@oregonstate.edu

in the flux estimates. A full inversion – with the same or an independent 'prior' land flux – translates observation residuals into modifications to surface fluxes and this process provides additional information from the CO_2 concentration observations. Here, we take this forward mode approach to evaluate a bottom-up NEE flux estimate for North America that includes component fluxes not previously treated in an inversion framework.

Net ecosystem exchange is the most relevant flux term to use in the context of integrating bottom-up and top-down scaling approaches because NEE is what an atmospheric inversion 'sees'. The term refers specifically to the vertical flux of CO_2 over a specified area and interval (Chapin *et al.*, 2006). By the convention of atmospheric scientists, a positive sign on a flux estimate is a transfer of carbon into the atmosphere. At the ecosystem scale, NEE consists primarily of NEP, the balance of net primary production and heterotrophic respiration (here the convention among ecologists is that a positive sign indicates transfer of carbon into the ecosystem). However, at the regional scale additional components of NEE include emissions associated with wildfire, respiration of harvested forest and agriculture products, and CO_2 evasion from water bodies (Hayes & Turner, 2012).

Studies at eddy covariance (EC) tower sites suggest that the range of NEP (i.e., −NEE) across all ecosystems is on the order of 800 to −200 gC m^{-2} yr^{-1} (Yi *et al.*, 2010). Its magnitude is impacted by environmental gradients (Yi *et al.*, 2010), interannual variation in climate (e.g., Reichstein *et al.*, 2007), and the disturbance regime (Luyssaert *et al.*, 2007; Amiro *et al.*, 2010). Croplands are expected to be NEP sinks because much of the net primary production is removed with the harvest and only crop residues are left to generate heterotrophic respiration (Gilmanov *et al.*, 2013). Young forests are typically also large carbon sinks, whereas old forests are more nearly carbon neutral and recently disturbed forests can be carbon sources (Amiro *et al.*, 2010; Coursolle *et al.*, 2012). The possibilities for simulating NEP over large domains have improved in the last decade by development of satellite-based datasets for mapping land cover and monitoring vegetation greenness (Justice *et al.* 2002), as well as expansion of the network of EC flux towers capable of continuously monitoring carbon flux (Baldocchi *et al.*, 2001). However, there is general recognition that heterotrophic respiration is often underestimated in forests when upscaling tower fluxes because of limited information about the disturbance regime (Jung *et al.*, 2011). In this study, we simulate NEP by upscaling EC tower observations, but include forest stand age in our NEP algorithm to better account for past disturbance.

The source of CO_2 from biomass burning includes both wildfire (French *et al.*, 2011) and crop residues (McCarty *et al.* 2009). For the purposes of developing a daily emissions estimate at the continental scale, active fire area is monitored by remote sensing (Giglio *et al.* 2009) and emissions are estimated based on biomass and combustion factors. Biomass is commonly simulated with a process-based productivity model (Van der Werf *et al.*, 2006). The degree to which the carbon source from biomass burning offsets NEP carbon sinks is relatively low in most temperate forest areas (e.g., Turner *et al.* 2007), but may balance NEP over large areas of boreal forest (Bond-Lamberty *et al.*, 2007; Hayes *et al.*, 2011).

Evasion of CO_2 from rivers and streams is increasingly recognized as an important component of NEE (Cole *et al.*, 2007; Luyssaert *et al.*, 2012), but has not generally been included in spatially explicit bottom-up NEE scaling efforts. The source of the CO_2 in first-order streams is predominantly inorganic and organic carbon swept out of the soil in the soil solution, whereas in large rivers it is predominantly respiration of allochthonous organic matter (Butman & Raymond, 2011). When NEP is based on upscaled tower fluxes, the dissolved inorganic carbon and organic carbon that is carried to streams in the soil solution (along with the organic particulate matter deposited to the water surface) has for the most part been 'seen' going into the ecosystem when EC-based NEE was measured. Such would also be the case for the small proportion of river/stream evasion (ca. 10%, Ciais *et al.*, 2008) that originates in the process of mineral weathering and is likewise carried in the soil solution. Therefore, at the regional scale, river evasion should be added to upscaled tower fluxes to get total NEE.

The carbon source from harvested forest and crop products is also beginning to be included in regional carbon budgets (Ciais *et al.*, 2008), but generally not in a spatially explicit manner. The crop harvests are exported internationally or consumed by humans and livestock, and emitted over the course of the following year. The forest harvests are returned to the atmosphere at varying rates in the form of direct emissions during wood processing and slower release from landfills after product disposal (Heath *et al.*, 2011). For North America, we now have the opportunity to include this flux in a spatially explicit form. Hayes *et al.* (2012) collected crop and forest inventory data for Canada, the United States, and Mexico and assembled the harvested product source data in a spatially distributed format.

In this study, NEP was simulated by upscaling carbon fluxes from EC flux towers (King *et al.*, 2012), fire carbon sources were based on remote sensing and ecosystem modeling (Van der Werf *et al.*, 2006), harvested product sources were derived from inventory data (Hayes *et al.*, 2012), and evasion of CO_2 from aquatic bodies was estimated by an empirical relationship between observed fluxes and precipitation (Butman & Raymond, 2011). This NEE was run in the forward mode through the CarbonTracker inversion setup (Peters *et al.*, 2007, http://carbontracker.noaa.gov) using the TM5 atmospheric transport model, and residual errors in predicted CO_2 concentration were examined. The spatial and temporal patterns in NEE from the bottom-up approach and a full CarbonTracker inversion with an independent prior flux were also compared. Our approach permitted a more highly disaggregated diagnosis of the absolute land flux over North America than has been previously achieved, along with its evaluation in an aggregate form.

Our NEE scaling and evaluation approach makes use of five extensive observational datasets: (i) a network of meteorological stations for development of spatially distributed climate to drive a bottom-up NEP model (Nemani *et al.* 2009); (ii) measurements of vegetation status from satellite-borne sensors to drive the bottom-up NEP model and detect burned area (Justice *et al.* 2002); (iii) measurements of ecosystem-level carbon fluxes from the global network of EC flux towers to parameterize the NEP model (Baldocchi *et al.*, 2001); (iv) measurements of atmospheric CO_2 concentration as reference data in the inversion setup (Conway *et al.*, 1994); and (v) measurements of carbon stocks and flux at networks of field plots associated with national-level forest and crop inventories to estimate harvested products emissions and to map forest stand age (Pan *et al.* 2011; Hayes *et al.*, 2012). The impediments to integrated use of these data include definitional differences between disciplines, incompatible spatial and temporal scales between top-down and bottom-up modelers, and inconsistencies among driver datasets (Hayes & Turner, 2012; Huntzinger *et al.*, 2012). The benefits lie in improved constraints on the net flux estimates and better understanding of the component fluxes (Running *et al.*, 1999; Turner *et al.*, 2011a).

Materials and methods

Overview

Daily fluxes for 2004 were assembled for each of the four NEE components. These data were spatially aggregated to the one degree resolution of CarbonTracker, and subsequently temporally disaggregated to its 3 hourly time step. The fluxes were then run in the forward mode through CarbonTracker, with fossil fuel emissions and CO_2 boundary conditions for North America provided by the standard CarbonTracker setup. The residuals between observed and simulated CO_2 concentration (mixing ratio) at eight observation sites in North America were used to evaluate the bottom-up NEE simulations.

Scaling net ecosystem production

The CFLUX diagnostic carbon cycle model (Turner *et al.*, 2006) was run in a spatially distributed mode to simulate NEP (Fig. 1). The model algorithms and evaluation are described in detail elsewhere (Turner *et al.*, 2006, 2009; King *et al.*, 2011). The model uses a daily time step, and for this study was applied at the 1 km spatial resolution. Gross primary production (GPP) is estimated with a light use efficiency (LUE) approach in which GPP is the product of absorbed photosynthetically active radiation (APAR) and an estimate of LUE (gC MJ^{-1}). APAR is derived from incoming PAR and the fraction of PAR absorbed by the vegetation canopy (FPAR). The LUE is estimated based on a plant functional type (PFT)-specific clear-sky LUE (from EC flux tower observations), which is upregulated by a cloudiness index and downregulated by scalars for minimum temperature, vapor pressure deficit (VPD), soil moisture, and stand age (in the case of forests). Autotrophic respiration is a PFT-specific proportion of GPP. Heterotrophic respiration (R_h) is a function of a base rate and scalars for soil temperature (Lloyd and Taylor 1994), soil moisture, FPAR, and stand age (in the case of forests). The model maintains a simple soil water balance by reference to a PFT-specific water use efficiency parameter (mm H_2O per gC of GPP).

The daily meteorological inputs (PAR, minimum temperature, maximum temperature, VPD, and precipitation) for the NEP model were from interpolated meteorological station data at the 8 km spatial resolution (Wang *et al.*, 2010). Soil water holding capacity (WHC) was prescribed by PFT based on representative values at flux tower sites (King *et al.*, 2011). This approach was taken after running the analysis with a

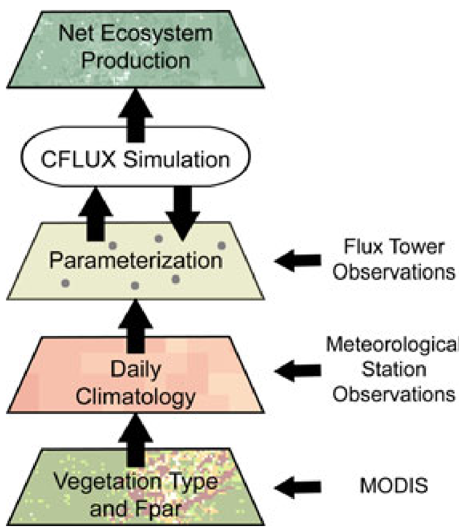

Fig. 1 Bottom-up net ecosystem production (NEP) modeling approach.

distributed WHC dataset Global Soil Data Task Group (GSDTG, 2000) and finding significant grassland areas which ran out of water in the simulation, but showed no influence of drought in their FPAR. PFT (Fig. 2a) was from the standard Collection 5 MODIS product (Friedl *et al.*, 2010; LP DAAC, 2012) and climate zones from aggregations of the Omernik (1987) ecozones (Fig. 2b). The FPAR was likewise derived from the Collection 5 MODIS product (Myneni *et al.*, 2002; LP DAAC, 2012) with gap filling using the algorithm of Zhao *et al.* (2005). Forest stand age (Fig. 4b) was from the 1 km resolution product of Pan *et al.* (2011). That product included only Canada and the US, so approximations (50–100 years) were made for the various forest types in Mexico. Irrigated areas (Fig. 3b) were from GSDTG (2000).

The CFLUX parameter optimization procedure for North America is described in King *et al.* (2011). For each combination of PFT (n = 7) and climate zone (n = 3) that included a substantial area, observations of gross ecosystem exchange GEE (−GPP) and NEE from one or more EC flux tower sites having the same PFT and climate zone were obtained from AmeriFlux (2013) or directly from the tower operator. In the case of temperate grasslands, we added an additional northern and southern region breakout because of the extreme temperature range associated with that PFT/climate zone combination. The final grassland parameters were also adjusted such that the total 2004 NEP for the Great Plains approximated the comparable estimate from the detailed study by Zhang *et al.* (2011). We used the same distributed climate and FPAR data in the optimizations that was later used in the spatial mode run of the model.

The cost function in the optimizations was the root mean square error (RMSE) for the observed GPP and NEP fluxes at the daily time step (Moore & McCabe, 2006). Optimized parameters included (i) the minimum and maximum temperature and minimum and maximum VPD that controlled the temperature and VPD scalars in the GPP algorithm; (ii) the maximum LUE; (iii) the base rate of R_h; (iv) a parameter that controlled the sensitivity of R_h to soil temperature; and (v) a parameter that set a minimum for the FPAR scalar outside the growing season (Turner *et al.*, 2006, 2009; King *et al.*, 2011). A minimum estimate for the effect of model error on the uncertainty of the total annual NEP reported here for NA was calculated as product of the RMSE for annual NEP across all EC tower sites used in the parameter optimization exercise of King *et al.* (2011) and the vegetated area of North America. Evaluating additional uncertainties associated with model structure, distributed model inputs (notably climate, FPAR, and stand age), and the EC flux measurements used as reference observations in the parameter optimizations was beyond the scope of this study.

Additional CO_2 Sources

Fire emissions. Daily emissions from biomass burning were from Van der Werf *et al.* (2006). Fire extent in that study was from the MODIS Active Fire and MODIS Burned area products. Fuel loads were from the CASA ecosystem process model run in a spatially distributed mode, and emission factors (proportion of fuel burned) were from the literature. This fire emissions database (CASA-GFED3) is the same as is used in the standard CarbonTracker inversion (CT2011, 2011).

River/stream evasion. Butman & Raymond (2011) estimated river/stream evasion over North America based on measurements of temperature, alkalinity, and pH along with high-resolution data on morphology and surface area of waterways. Aggregation of their data to the regional scale resulted in a

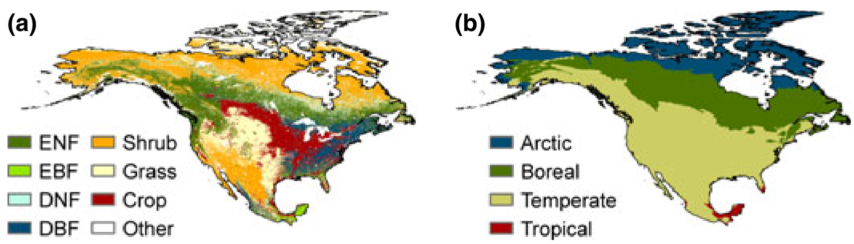

Fig. 2 The study domain: (a) plant functional types, (b) climate zones. ENF, evergreen needle leaf forest; EBF, evergreen broadleaf forest; DNF, deciduous needle leaf forest; DBF, deciduous broadleaf forest.

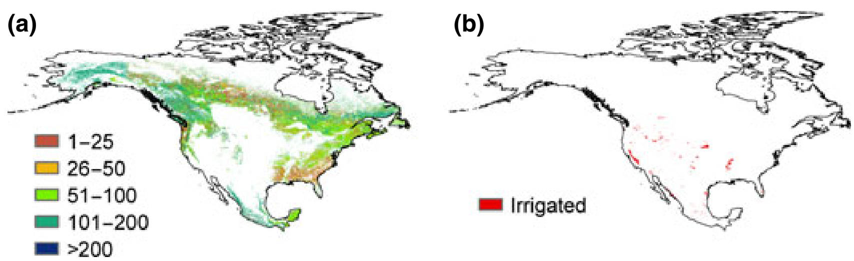

Fig. 3 Land surface characteristics: (a) forest stand age, (b) irrigation status.

strong linear relationship of annual precipitation to annual river/stream evasion. We used that linear relationship and our annual precipitation (8 km resolution) to map annual evasion emissions. To partition the annual data to the daily time step, all days with soil temperature ≤0 °C were flagged. The annual total was then partitioned among the remaining days based on their daily precipitation.

Harvested products. In Hayes *et al.* (2012), an inventory approach was used to estimate annual emissions from harvested wood products and crops. These fluxes were spatially resolved to the level of political units such as states or provinces. For our daily flux at 1 km, the polygon maps based on data from Hayes *et al.* (2012) were resampled to 1 km resolution and linearly interpolated over the course of the year. Product emissions data were not available for Mexico.

The CarbonTracker setup

CarbonTracker release version 2011_oi (Fig. 4, henceforth CT2011, 2011) is updated from Peters *et al.* (2007) as described at the CarbonTracker web site (http://carbontracker.noaa.gov/CT2011). Here, we used the forward mode to predict CO_2 concentrations for comparison with observations. CarbonTracker employs the TM5 transport model and operates at the spatial resolution of 1 degree over North America using 3 hourly meteorological fields from the European Centre for Medium-range Weather Forecasts (ECMWF) operational weather prediction model. We aggregated our daily land fluxes to the 1 degree resolution by spatial averaging. They were then disaggregated temporally to the 3 h time step (Olsen & Randerson, 2004): daily GPP was distributed over the daylight hours based on proportionality to the modeled shortwave radiation, and daily ecosystem respiration (+ product and river/stream evasion sources) was distributed over the day by assuming that it is proportional to the Q_{10} computed from near-surface air temperature.

The CO_2 boundary conditions for North America as well as the global fossil fuel emissions and fire emissions were from the CT2011, 2011_oi product, with the CASA-GFED3 carbon cycle process model providing the prior land flux. The Carbon Tracker inversion uses a global network of CO_2 observational datasets in its cost function. For the purposes of evaluating our bottom-up NEE, we examined the CO_2 concentration residuals at a set of eight sites in the CarbonTracker network that were likely to be impacted by the North America fluxes (Fig. 5). Specifics on site characteristics, CO_2 measurement protocols, and uncertainty assessment are given in Andrews *et al.* (2013). The reference concentrations were means over the 12:00 to 16:00 period of local time. For comparison, we also examined the same residuals from a forward mode run using one of the alternate CarbonTracker priors (CASA-GFED3$_{EVI}$, CT2011, 2011). In addition, we overlaid in space and time our annual bottom-up NEE and the posterior NEE from the standard CarbonTracker inversion ensemble. Inversion uncertainty was specified based on runs with eight different transport models. Additional uncertainties, e.g., associated with CO_2 measurements and alternative priors, are not treated here.

Results

Net ecosystem production

Total NEP for North America in 2004 was estimated at 1730 TgC yr^{-1} using our diagnostic modeling approach (Fig. 6a). Uncertainty in the annual total NEP associated with the model and its parameters is estimated at 370 TgC yr^{-1}. As noted, additional uncertainty not quantified here is associated with representativeness of the EC tower optimization sites (King *et al.*, 2011), EC tower flux measurements themselves (Moffat *et al.*, 2007), the meteorological driving data (Wang *et al.*, 2010), and the FPAR driving data (Turner *et al.*, 2005).

The largest contributors to the total NEP (i.e., sinks of over 100 TgC yr^{-1}) were from the temperate crop and temperate broadleaf forest vegetation classes (Table 1). Both had high mean sink rates and large areas. Temperate evergreen needle leaf forest (ENF) and boreal deciduous broadleaf forest (DBF) had moderate mean NEPs and lower areas, but nevertheless each generated a sink

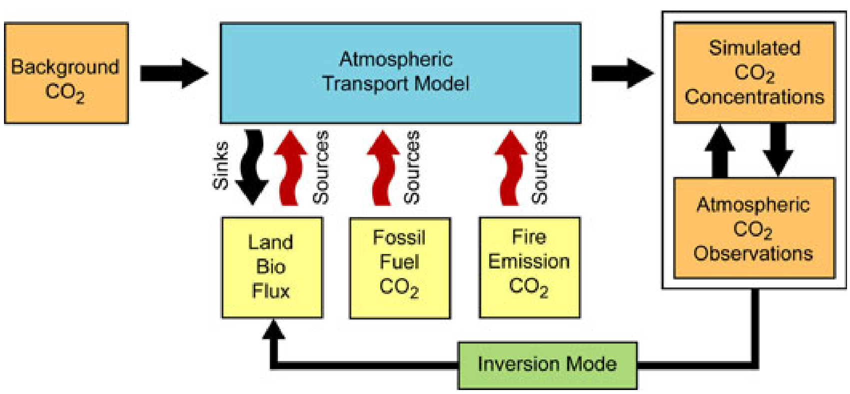

Fig. 4 Top-down net ecosystem exchange (NEE) modeling approach. NEE is the sum of land biologically driven flux and fire emissions.

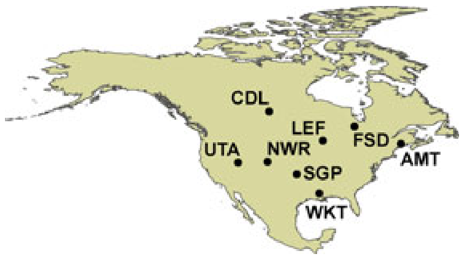

Fig. 5 Sites used to evaluate CO_2 prediction errors. Site acronyms as in CT2011 (2011).

greater than 70 TgC yr^{-1}. Boreal ENFs were a significant sink, driven more by a large area than a high mean uptake. Temperate and boreal shrubs likewise had large areas, but low mean NEP. Tropical croplands had the highest mean sink but a relatively small area. Temperate grasslands in sum were a sink of over 100 TgC yr^{-1}, mostly because of a large area. There were limited source areas in grasslands of the southern Great Plains, in regions of extreme heat or cold, and in dispersed grid cells of very young forests.

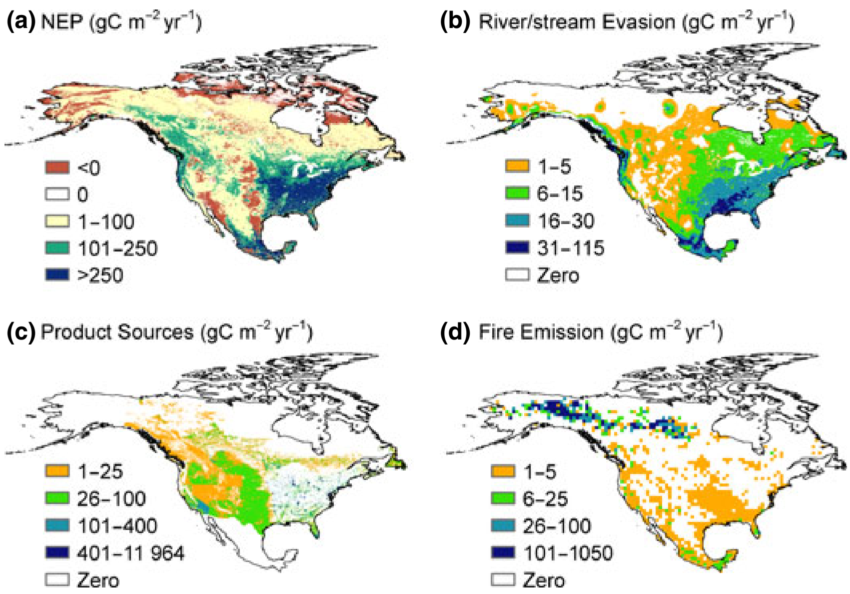

Fig. 6 Bottom-up fluxes: (a) net ecosystem production (NEP), (b) river/stream evasion, (c) product sources, (d) fire.

Table 1 CFLUX Net Ecosystem Production (NEP) by plant functional type/climate zone combination

Climate Zone	PFT*	Area (km^2)	Mean NEP (gC m^{-2} yr^{-1})	Total NEP (TgC yr^{-1})
Temperate	DBF	1 239 791	297	461
Temperate	Crop Broadleaf	1 240 330	249	295
Temperate	Crop Cereal	1 272 356	164	185
Temperate	ENF	1 163 391	139	181
Boreal	ENF	2 077 204	47	120
Temperate	Grass	2 867 188	42	123
Boreal	DBF	645 547	135	90
Temperate	Shrub	2 206 077	36	80
Tropical	Crop Broadleaf	78 001	413	38
Boreal	Shrub	1 501 020	16	26
All other		4 749 511	4	131
TOTAL		19 040 416		1730

DBF, deciduous broadleaf forest; ENF, evergreen needle leaf forest.
*Plant functional type (PFT) designations as in Fig. 2a.

Stand age was a significant influence on NEP at all scales. In the forests of the Southeast US, which are largely managed for wood production, the mean stand age over the states of Louisiana, Alabama, Mississippi, and Georgia was 42 years, and the mean NEP was 263 gC m^{-2} yr^{-1}. Much of the DBF in the Northeastern US. is recovering from use as marginal agriculture (Fuller *et al.* 1998), hence the mean stand age in forestland of the state of Massachusetts was relatively young (89 years) and the mean NEP was 284 gC m^{-2} yr^{-1}. In a sensitivity test in which stand age was fixed at ages of 25, 100, or 250 years over the entire range of forests in North America, our summed NEPs for 2004 were 2165, 1660, and 1011 TgC yr^{-1}, respectively.

Additional CO_2 sources

Harvested products. The total product source was 316 TgC yr^{-1}, with a spatial distribution largely following the distribution of livestock and people (Fig. 6c). Highest source areas were thus in large cities, in the Great Plains of the US, and in southern California. The linear features in the flux map are the result of geopolitical boundaries associated with the reporting units for agricultural products. Uncertainty on the estimate for harvested product emissions for NA is on the order of 80 TgC yr^{-1} (Hayes *et al.*, 2012).

River/stream evasion. The total river/stream evasion source for 2004 was 158 TgC yr^{-1}, with an uncertainty estimate on the order of 49 TgC yr^{-1} based on the uncertainty analysis of Butman & Raymond (2011). The highest modeled fluxes were associated with areas of high precipitation in the temperate and tropical zones (Fig. 6b). The Butman & Raymond (2011) function relating annual emissions to annual precipitation has an intercept at 200 mm, so our emissions estimate was zero over large areas at high latitudes where annual precipitation in 2004 fell below that value.

Fire emissions. Total fire emissions in 2004 were estimated at 142 TgC yr^{-1} (Fig. 6d). We approximated uncertainty at ±45 TgC yr^{-1} based on independent bottom-up and top-down analyses (Kopacz *et al.*, 2010; Hayes *et al.*, 2011). The largest source areas were boreal Alaska and Canada as well as lowland forests in western Mexico and the Yucatan Peninsula.

Net ecosystem exchange

The total bottom-up NEE estimate for NA in 2004 was −1115 TgC yr^{-1}, with an estimation range from −899 to −1364 TgC yr^{-1} based on the component flux uncertainties (Table 2). The largest component term was NEP, followed by products, river/stream evasion, and fire. The agricultural areas of the US Midwest and the DBFs in the eastern portion of the country were large NEE sinks. Forest areas in the Pacific Northwest and Southeastern US were moderate sinks. Midcontinent grasslands were a carbon source, primarily driven by crop-related emissions. The combination of sources from harvested products, river/stream evasion, and fire constituted a 35% offset to the NEP sink.

Table 2 Net ecosystem exchange (NEE) flux components and ranges for North America in 2004. Units are TgC yr^{-1}

Component	Best estimate	Low	High
Net ecosystem production (sink)	1730	1359	2162
River/stream evasion (source)	158	109	207
Harvested products (source)	316	246	396
Fire emissions (source)	142	105	195
Total NEE	1115	899	1364

CarbonTracker diagnostics

When the bottom-up NEE was run in the forward mode with the TM5 transport model, there was virtually no bias in the winter, but a positive bias (1.58 μmol mol^{-1} CO_2) in predicted concentrations in the summer across our eight reference measurement sites (Fig. 7). The Wisconsin LEF tower, which samples a large area of managed forests and farmland in the mid-west US, clearly shows the summer bias (Fig. 8). This pattern suggests a tendency to underestimate summer NEE sinks. The CASA-GFED3$_{EVI}$ prior used in the CarbonTracker inversion (CT2011, 2011) showed a larger positive bias in the summer (3.22 μmol mol^{-1} CO_2), but also a positive bias (1.48 μmol mol^{-1} CO_2) in the winter – suggesting too large a source.

The total posterior NEE for the full CarbonTracker inversion was −953 TgC yr^{-1}, 15% lower (i.e., less of a carbon sink) than the bottom-up NEE. The uncertainty based on alternative transport models was 106 TgC yr^{-1}.

Comparison of the geographic pattern in NEE for the bottom-up and top-down approaches here (Fig. 9; Table 3) indicates broad areas of agreement in terms of the sign of the flux, particularly with regard to an extensive carbon sink in the croplands of the Midwest US. There was disagreement in the magnitude of the carbon sink for most temperate forests, with higher values using the bottom-up approach. In the southern Great Plains, there were source areas only in the case of the bottom-up approach. The frequency distributions for annual NEE in the 1° grid cells (Fig. 10) were similar in that both showed a maximum in the

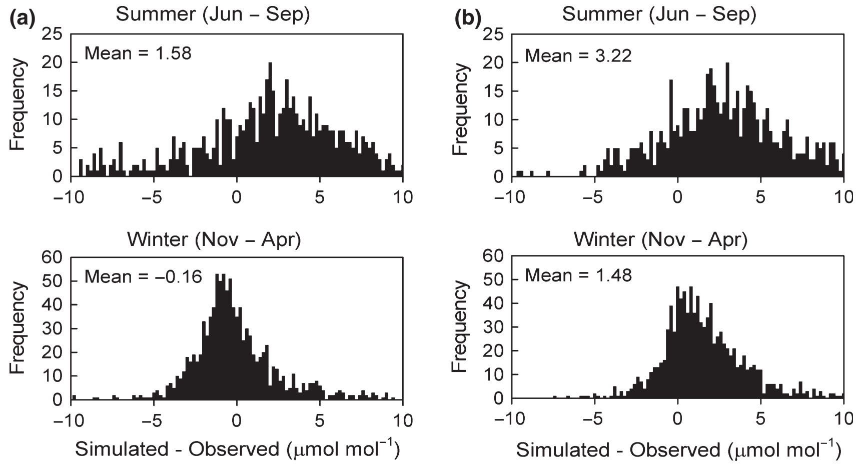

Fig. 7 Frequency distributions for residuals of simulated CO_2 concentration at eight measurement sites in North America. Values outside the −10 to 10 μmol mol^{-1} range are treated as outliers. (a) bottom-up approach with net ecosystem production (NEP) from CFLUX, (b) forward model approach with land biologically driven flux from CASA-GFED$_{EVI}$.

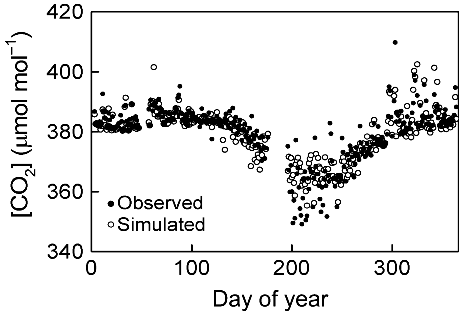

Fig. 8 Comparison of observed and simulated CO_2 concentrations at the LEF site in Wisconsin.

Table 3 Net ecosystem exchange (NEE) by plant functional type and climate zone for top-down and bottom-up scaling approaches. Values are mean NEE in gC m^{-2} yr^{-1}

Climate zone	PFT*	Top-down	Bottom-up
Temperate	DBF	−90	−253
Temperate	Crop Broadleaf	−144	−205
Temperate	Crop Cereal	−119	−123
Temperate	ENF	−11	−104
Boreal	ENF	−29	−14
Temperate	Grass	−72	−1
Boreal	DBF	−89	−112
Temperate	Shrub	−19	−9
Tropical	Crop Broadleaf	−95	−380
Boreal	Shrub	−16	2
All other		−14	−4

DBF, deciduous broadleaf forest; ENF, evergreen needle leaf forest.
*Plant functional type (PFT) designations as in Fig. 2a.

0 to −50 gC m^{-2} yr^{-1} bin. However, the bottom-up approach had more cells that were sources and its distribution extended to a larger range of NEE sinks.

In the temporal domain, the time series for daily mean NEE over North America (Fig. 11) showed an earlier transition from source to sink in the spring for the bottom-up approach (i.e., crossing the 0 NEE line around day 102 compared to day 116 for the inversion). There was an earlier return from sink to source in the case of the inversion (day 256 vs. day 270). The peak summertime uptake strength was 63% greater for the inversion, whereas wintertime sources were of a similar magnitude.

Discussion

Net ecosystem production

The climate over North America in 2004 was largely favorable to NEP sinks. The west coast mountainous regions were relatively warm, whereas the continental interior was relatively cool and wet (Levinson, 2005). Both corn and soybean in the Midwest United States have recorded high levels of productivity per unit area (USDA, 2005). At a mixed hardwood/conifer forest site in eastern North America, NEE measured by the EC approach (equivalent to – NEP) was −410 gC m^{-2} yr^{-1} in 2004 compared to a 10 year average of −242 gC m^{-2} yr^{-1} (Urbanski *et al.*, 2007). EC studies at several boreal and temperate zone conifer sites in North America also found the NEE carbon sink to be the highest or among the highest in their multiyear records (Dunn *et al.*, 2007; Krishnan *et al.*, 2009; Thomas *et al.*, 2009). The area that is a notable exception is interior Alaska where unusually warm and dry conditions

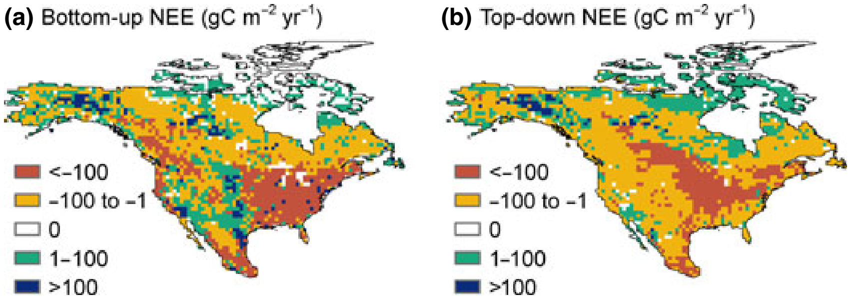

Fig. 9 Net ecosystem exchange using (a) bottom-up and (b) top-down approaches.

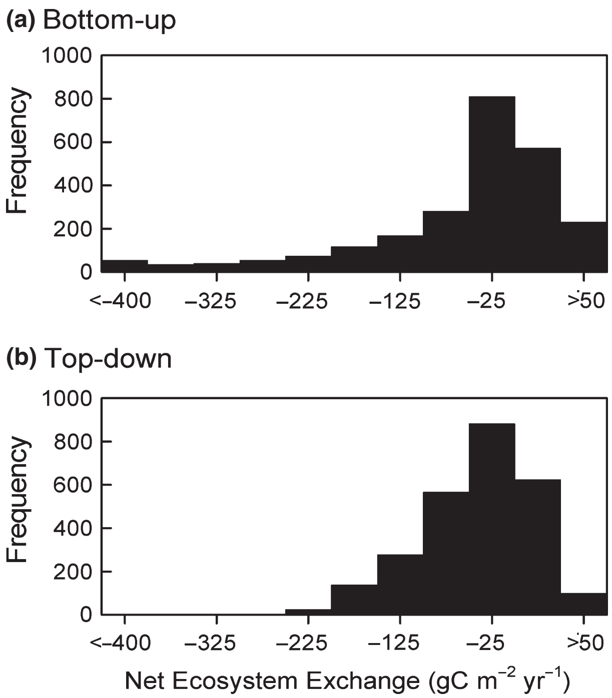

Fig. 10 Frequency distributions for mean net ecosystem exchange within 1° grid cells over North America: (a) bottom-up approach, (b) top-down approach. The bin interval is 50 gC m^{-2} yr^{-1} and the *x*-axis values represent the bin midpoints.

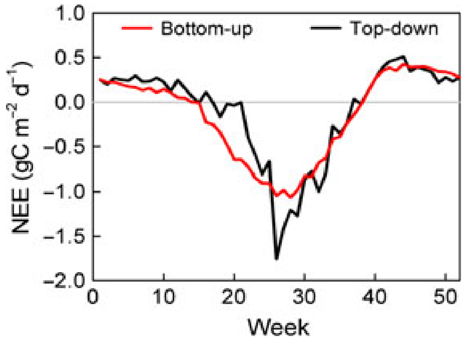

Fig. 11 Time series of daily mean net ecosystem exchange at weekly intervals over the North America domain.

reduced carbon sinks in 2004 (Welp *et al.* 2007). Other bottom-up studies suggest NEPs of similar magnitude (Table 4) and three studies besides the present one that upscaled EC data over all or large parts of North America reported 2004 as a relatively high NEP sink year (Chen *et al.*, 2011; Sun *et al.*, 2011; Zhang *et al.*, 2011).

Scaling NEP with CFLUX was based on stratifying the land base by climate zone and PFT. With respect to optimizing parameters such as LUE, many studies have supported the use of PFT-specific parameters in diagnostic models (Turner *et al.*, 2005; Xiao *et al.*, 2005; Gilmanov *et al.*, 2013). Here, we added stratification by climate zone, which may be particularly pertinent in the case of grasslands because this PFT extends across an exceedingly broad range of temperatures. Conifer forests likewise occur across a wide environmental gradient, and comparisons across EC tower sites suggest a more conservative metabolism (e.g., lower LUE) in the case of boreal forests (Garbulsky *et al.*, 2010). This observation may best be captured in a distributed NEP model by a PFT × climate zone stratification.

Several studies based on upscaling EC tower data have pointed to the importance of including disturbance effects (Desai *et al.*, 2005; Jung *et al.*, 2011; Xiao *et al.*, 2012). Here, we used a stand age product (Pan *et al.*, 2011) that was based on the Landsat record to capture fires in recent decades. The ages of older stands (based on inventory data) were also used in that product, but were spatially explicit to a lesser degree. Thus, there were undoubtedly mismatches of stand age and FPAR in some cases. The scale of the disturbance regime's spatial heterogeneity is also an issue in that management units in heavily managed forest areas are often smaller than the 1 km^2 of the FPAR data (Turner *et al.*, 2000). Future scaling efforts could make greater use of Landsat data for stand age (e.g., Duane *et al.*, 2010), and potentially take advantage of stand height mapping efforts based on satellite-borne lidar instruments as an indicator of time since disturbance (Lefsky 2010).

Table 4 Flux estimates for North America. Values are TgC yr^{-1}

Flux type	Domain	Estimate	Uncertainty*	Year(s)	Reference
NEP	United States	730†	180	2004	Chen *et al*. (2011)
		1111†	237	2004	This study
		1210†	NA	2001–2006	Xiao *et al*. (2011)
		2703†	2282	2001–2006	Sun *et al*. (2011)
NEE	United States	500‡	400	2004–2006	Crevoisier *et al*. (2010)
		717†	299	2004	This study
	N. America	570‡§	NA	2004	Schuh *et al*. (2010)
		953‡	106	2004	CT2011, 2011;
		1050‡	300	2004	Gourdji *et al*. (2012)
		1115†	465	2004	This study
		1230‡	1120	2001–2003	Butler *et al*. (2010)

NA, not available; NEE, net ecosystem exchange; NEP, net ecosystem production.
*Uncertainties are based on a variety of approaches and not directly comparable.
†Bottom-up approach.
‡Top-down approach.
§Does not include Mexico and Alaska.

Additional CO_2 sources

Products. As with fire and river/stream evasion, the NEE based on upscaled tower fluxes sees the carbon associated with harvested products as it is taken up in croplands and managed forests, but does not see the lateral transfer of the harvested products away from those ecosystems (Ciais *et al*., 2008; Hayes *et al*., 2012; Gilmanov *et al*., 2013). The large magnitude of the products source helps explain how mean NEP can be quite high for some regions, whereas continental scale total NEE is much lower.

River and stream evasion. Our estimate for river and stream evasion from the conterminous US. (94 TgC yr^{-1}) using a simple precipitation-based algorithm was consistent with the flux estimate for the US. (97 TgC yr^{-1}) from the more detailed study on which our algorithm was based (Butman & Raymond, 2011). The magnitudes are also in good agreement with estimates from detailed catchment scale studies such as Wallin *et al*. (2012). The strength of the precipitation/evasion relationship is likely based on the flushing effect of high precipitation and the link of high precipitation to high vegetation productivity. It is apparent that in evaluating continental scale NEE, river/stream evasion is a significant term (Cole *et al*., 2007).

Fire. The area burned in forests of western Canada and Alaska was relatively high in 2004 (Turquety *et al*., 2007) in association with an exceptionally warm and dry April–July (Levinson, 2005). The CASA-GFED3-based estimate for fire emissions in 2004 over North America was the highest over the 2000–2010 interval (CT2011, 2011). However, even that is likely an underestimate. Hayes *et al*. (2011) suggested a source of 200 TgC yr^{-1} for just boreal North America in 2004, and the CASA-GFED3 source estimates in western Canada for 2010 are believed to be underestimated by 30% based on an inversion using observations of CO concentration (Kopacz *et al*., 2010). If indeed fire emissions in 2004 were higher than 142 TgC yr^{-1}, it would reduce our bottom-up estimate of the NEE sink by a corresponding amount.

Bottom-up net ecosystem exchange

Adding emission from fire, river/stream evasion, and harvested products to NEP reduced the magnitude of the annual carbon sink by about one third. As noted, 2004 appears to have been a relatively high NEP year for North America, thus the proportion of annual fossil fuel emissions offset by NEE over North America estimated here (62%) is likely at the high end of the interannual variation. Such was also the case for 2004 with NEE from the ensemble CarbonTracker inversion over the 2000–2010 interval (CT2011, 2011).

Evaluation with an atmospheric inversion model

The overprediction of CO_2 concentrations for the summer season when using our bottom-up approach could have several sources. First is that the simulated NEE sink in summer was underestimated. This pattern might be expected if the tower data with which the NEP model is calibrated tended to have a low sink bias. However, the opposite is more likely the case as an underestimate of ecosystem respiration due to low turbulence at nighttime or in the lower canopy is potentially a common bias in EC tower flux estimation (Van Gorsel *et al.*, 2009; Thomas *et al.*, 2013). Our CASA-$GFED3_{EVI}$ bottom-up fluxes are calibrated with a global set of net primary production measurements, and resulted in a similar overprediction of CO_2 concentration in the summer (Fig. 7b) – also suggesting insufficient summer uptake. Zhang *et al.* (2012) have pointed out that LUE models may generally underestimate GPP when FPAR is relatively high (and overestimate GPP when FPAR is low) because shade-lit foliage, in which photosynthesis is not light saturated, would have a higher LUE than sun-lit foliage.

An alternative interpretation of the overprediction of CO_2 in the summer is that the west coast boundary conditions for CO_2 could be high to begin with (Schuh *et al.*, 2010; Gourdji *et al.*, 2012). This was the case in Göckede *et al.* (2010), which compared measurements and CO_2 simulations from CarbonTracker at two sites in western Oregon. As CarbonTracker is a global model, a potential explanation of this is inadequate terrestrial uptake in Eurasia. We did not explicitly investigate this issue here. The transport model itself must also be considered. Stephens *et al.* (2007) found that many of the TRANSCOM transport models have vertical gradients that are too small in the North American summer, indicating that uptake signals are mixed away from the surface too vigorously. This implies that an inversion constrained by surface observations would have to estimate an erroneously large sink to correctly simulate low CO_2 concentrations. In forward mode simulations, overly strong vertical mixing with correct surface fluxes would manifest as simulated summertime surface CO_2 values that are higher than those observed. Distinguishing between faults of surface flux and atmospheric transport remains a major challenge in atmospheric CO_2 modeling.

The wintertime high bias in predicted concentrations with the CASA-$GFED3_{EVI}$ prior (Fig. 7b) could be a case of model overestimation of ecosystem respiration (or less likely underestimation of GPP), issues with boundary conditions for CO_2, or transport model underestimation of boundary layer height. CASA is spun-up to near carbon equilibrium (Olsen and Randolph 2004), whereas flux towers suggest many ecosystems are carbon sinks (Yi *et al.*, 2010), thus the CASA-GFE-$D3_{EVI}$ winter sources may be too high. Our bottom-up winter source is smaller, despite the added non-NEP sources, because of less ecosystem respiration.

The similarity of the NA annual sums for the bottom-up and top-down approaches could be reconciled if the inversion underestimated net sinks in forested areas and underestimated net sources in areas of dense humans and livestock populations. In the case of temperate DBF, the higher C sinks with the bottom-up approach are supported by multiple EC tower sites with NEE values in the range -100 to -500 gC m^{-2} yr^{-1} (e.g., Wilson & Baldocchi, 2001; Urbanski *et al.*, 2007). The EC measurements in temperate ENF are more variable, with observations of carbon sources in the case of recently disturbed stands (Krishnan *et al.*, 2009) and in very old stands for specific years (Wharton *et al.*, 2012). However, bottom-up studies in the Pacific Northwest region using Landsat remote sensing to map stand age, and the Biome-BGC model to estimate NEP and fire emissions, support strong regional sinks (Turner *et al*. 2007; Turner *et al.*, 2011b; Meigs *et al.*, 2011). Forest inventory data also suggest strong accumulation of bolewood carbon in the Pacific Northwest region, particularly on public land where harvest levels are relatively low (Alig *et al.*, 2006). In the southeastern US, where there are large tracts of heavily managed coniferous forests, detailed bottom-up analyses that account for stand age class distribution also support a significant NEP (and by inference NEE) sink (Masek & Collatz, 2006).

Acknowledgments

This research was supported by the NASA Terrestrial Ecology Program (NNX09AL51G). Data from the AmeriFlux and FluxNet networks, the Biogeochemical Dynamics Distributed Active Archive Center, and the Land Processes Distributed Active Archive Center were essential for its completion. M. Zhao (University of Maryland) generously provided the filled MODIS Collection 5 FPAR product. We thank Arlyn Andrews and Ed Dlugokencky (NOAA Earth System Research Laboratory) and Doug Worthy (Environment Canada) for coordination of the CO_2 measurement networks. NASA provided use of the NEX computing facility at the NASA Ames Laboratory.

References

Alig RJ, Krankin ON, Yost A *et al.* (2006) Forest carbon dynamics in the Pacific Northwest (USA) and the St. Petersburg region of Russia: comparisons and policy implications. *Climatic Change*, **79**, 335–360.

AmeriFlux (2013) Available at: http://public.ornl.gov/ameriflux/ (accessed 25 March 2013).

Amiro BD, Barr AG, Barr JG *et al.* (2010) Ecosystem carbon dioxide fluxes after disturbance in forests of North America. *Journal of Geophysical Research-Biogeosciences*, **115**, G00K02.

Andrews AE, Kofler JD, Trudeau ME *et al.* (2013) CO_2, CO and CH_4 measurements from the NOAA Earth System Research Laboratory's Tall Tower Greenhouse Gas Observing Network: instrumentation, uncertainty analysis and recommendations for future high-accuracy greenhouse gas monitoring efforts. *Atmospheric Measurement Technical Discussion*, **6**, 1461–1553.

Baldocchi D, Falge E, Gu L *et al.* (2001) FLUXNET: a new tool to study the temporal and spatial variability of ecosystem-scale carbon dioxide, water vapor, and energy flux densities. *Bulletin of the American Meteorological Society*, **82**, 2415–2434.

Bond-Lamberty B, Peckham SD, Ahl DE *et al.* (2007) Fire as the dominant driver of central Canadian boreal forest carbon balance. *Nature*, **450**, 89–92.

Butler MP, Davis KJ, Denning AS *et al.* (2010) Using continental observations in global atmospheric inversions of CO_2: North American carbon sources and sinks. *Tellus*, **62B**, 550–572.

Butman D, Raymond PA (2011) Significant efflux of carbon dioxide from streams and rivers in the United States. *Nature Geoscience*, **4**, 839–842.

Chapin FS, Woodwell GM, Randerson JT *et al.* (2006) Reconciling carbon-cycle concepts, terminology, and methods. *Ecosystems*, **9**, 1041–1050.

Chen M, Zhuang Q, Cook DR *et al.* (2011) Quantification of terrestrial ecosystem carbon dynamics in the conterminous United States combining a process-based biogeochemical model and MODIS and AmeriFlux data. *Biogeosciences*, **8**, 2665–2688.

Ciais P, Borges AV, Abril G *et al.* (2008) The impact of lateral carbon fluxes on the European carbon balance. *Biogeosciences*, **3**, 1529–1559.

Ciais P, Rayner P, Chevallier F *et al.* (2010) Atmospheric inversions for estimating CO_2 fluxes: methods and perspectives. *Climatic Change*, **103**, 69–92.

Cole JJ, Prairie YT, Caraco NF *et al.* (2007) Plumbing the global carbon cycle: integrating inland waters into the terrestrial carbon budget. *Ecosystems*, **10**, 171–184.

Conway TJ, Tans PP, Waterman LS *et al.* (1994) Evidence for interannual variability of the carbon-cycle from the National Oceanic and Atmospheric Administration Climate Monitoring and Diagnostics Laboratory Global Air Sampling Network. *Journal of Geophysical Research-Atmospheres*, **99**, 22831–22855.

Coursolle C, Margolis HA, Giasson MA *et al.* (2012) Influence of stand age on the magnitude and seasonality of carbon fluxes in Canadian forests. *Agricultural and Forest Meteorology*, **165**, 136–148.

Crevoisier C, Sweeney C, Gloor M, et al. (2010) Regional US carbon sinks from three-dimensional atmospheric CO_2 sampling. *Proceedings of the National Academy of Sciences of the United States of America*, **107**, 18348–18353.

CT2011 (2011) CarbonTracker. Version 2011_oi. Available at: http://www.esrl.noaa.gov/gmd/ccgg/carbontracker/ (accessed 25 March 2013).

Deng F, Chen JM (2011) Recent global CO_2 flux inferred from atmospheric CO_2 observations and its regional analyses. *Biogeosciences*, **8**, 3263–3281.

Desai AR, Bolstad PV, Cook BD *et al.* (2005) Comparing net ecosystem exchange of carbon dioxide between an old-growth and mature forest in the upper Midwest, USA. *Agricultural and Forest Meteorology*, **128**, 33–55.

Duane MV, Cohen WB, Campbell JL *et al.* (2010) Implications of alternative field-sampling designs on Landsat-based mapping of stand age and carbon stocks in Oregon forests. *Forest Science*, **56**, 405–416.

Dunn AL, Barford CC, Wofsy SC *et al.* (2007) A long-term record of carbon exchange in a boreal black spruce forest: means, responses to interannual variability, and decadal trends. *Global Change Biology*, **13**, 577–590.

French NHF, De Groot WJ, Jenkins LK *et al.* (2011) Model comparisons for estimating carbon emissions from North American wildland fire. *Journal of Geophysical Research-Biogeosciences*, **116**, G00K05.

Friedl MA, Sulla-Menashe D, Tan B *et al.* (2010) MODIS Collection 5 global land cover: algorithm refinements and characterization of new datasets. *Remote Sensing of Environment*, **114**, 168–182.

Fuller TL, Foster DR, Mclachlan TS, *et al.* (1998) Impact of human activity on regional forest composition and dynamics in central New England. *Ecosystems*, **1**, 76–95.

Garbulsky MF, Penuelas J, Papale D *et al.* (2010) Patterns and controls of the variability of radiation use efficiency and primary productivity across terrestrial ecosystems. *Global Ecology and Biogeography*, **19**, 253–267.

Giglio L, Loboda T, Roy DP, *et al.* (2009) An active-fire based burned area mapping algorithm for the MODIS sensor. *Remote Sensing of Environment*, **113**, 408–420.

Gilmanov TG, Wylie B, Tieszen LL *et al.* (2013) CO_2 uptake and ecophysiological parameters of the grain crops of midcontinent North America: estimates from flux tower measurements. *Agriculture, Ecosystems and Environment*, **164**, 162–175.

Göckede M, Turner DP, Michalak AM *et al.* (2010) Sensitivity of a subregional scale atmospheric inverse CO_2 modeling framework to boundary conditions. *Journal of Geophysical Research-Atmospheres*, **115**, D24112.

Gourdji SM, Mueller KL, Yadav V *et al.* (2012) North American CO_2 exchange: intercomparison of modeled estimates with results from a fine-scale atmospheric inversion. *Biogeosciences*, **9**, 457–475.

GSDTG (Global Soil Data Task Group) (2000) *Global Gridded Surfaces of Selected Soil Characteristics (IGBP-DIS). [Global Gridded Surfaces of Selected Soil Characteristics (International Geosphere-Biosphere Programme - Data and Information System)]. Data set*. Oak Ridge National Laboratory Distributed Active Archive Center, Oak Ridge, Tennessee, USA. Available at: http://www.daac.ornl.gov (accessed 25 march 2013). doi: 10.3334/ORNLDAAC/569

Hayes D, Turner D (2012) The need for "apples-to-apples" comparisons of carbon dioxide source and sink estimates. *EOS*, **93**, 404–405.

Hayes DJ, McGuire AD, Kicklighter DW *et al.* (2011) Is the northern high-latitude land-based CO_2 sink weakening? *Global Biogeochemical Cycles*, **25**, GB3018.

Hayes DJ, Turner DP, Stinson G *et al.* (2012) Reconciling estimates of the contemporary North American carbon balance among terrestrial biosphere models, atmospheric inversions, and a new approach for estimating net ecosystem exchange from inventory-based data. *Global Change Biology*, **18**, 1282–1299.

Heath LS, Smith JE, Skog KE *et al.* (2011) Managed forest carbon estimates for the US Greenhouse Gas Inventory, 1990-2008. *Journal of Forestry*, **109**, 167–173.

Huntzinger DN, Post WM, Wei Y *et al.* (2012) North American Carbon Program (NACP) regional interim synthesis: terrestrial biospheric model intercomparison. *Ecological Modelling*, **232**, 144–157.

Jung M, Reichstein M, Margolis HA *et al.* (2011) Global patterns of land-atmosphere fluxes of carbon dioxide, latent heat, and sensible heat derived from eddy covariance, satellite, and meteorological observations. *Journal of Geophysical Research-Biogeosciences*, **116**, G00J07.

Justice CO, Townshend JRG, Vermote EF, *et al.* (2002) An overview of MODIS Land data processing and product status. *Remote Sensing of Environment*, **83**, 3–15.

King DA, Turner DP, Ritts WD (2011) Parameterization of a diagnostic carbon cycle model for continental scale application. *Remote Sensing of Environment*, **115**, 1653–1664.

King AW, Hayes DJ, Huntzinger DN *et al.* (2012) North American carbon dioxide sources and sinks: magnitude, attribution, and uncertainty. *Frontiers in Ecology and the Environment*, **10**, 512–519.

Kopacz M, Jacob DJ, Fisher JA *et al.* (2010) Global estimates of CO sources with high resolution by adjoint inversion of multiple satellite datasets (MOPITT, AIRS, SCIAMACHY, TES). *Atmospheric Chemistry and Physics*, **10**, 855–876.

Krishnan P, Black TA, Jassal RS *et al.* (2009) Interannual variability of the carbon balance of three different-aged Douglas-fir stands in the Pacific Northwest. *Journal of Geophysical Research-Biogeosciences*, **114**, G04011.

Lefsky MA (2010) A global forest canopy height map from the Moderate Resolution Imaging Spectroradiometer and the Geoscience Laser Altimeter System. *Geophysical Research Letters*, **37**, L15401.

Levinson DH (ed.) (2005). State of the climate in 2004. *Bulletin American Meteorological Society*, **86**, S1–S86.

Lloyd J, Taylor JA (1994) On the temperature-dependence of soil respiration. *Functional Ecology*, **8**, 315–323.

LP DAAC (2012) Land Processes Distributed Active Archive Center. Available at: https://lpdaac.usgs.gov/ (accessed 25 March 2013).

Luyssaert S, Inglima I, Jung M *et al.* (2007) CO_2 balance of boreal, temperate, and tropical forests derived from a global database. *Global Change Biology*, **13**, 2509–2537.

Luyssaert S, Abril G, Andres R *et al.* (2012) The European land and inland water CO2, CO., CH4 and N2O balance between 2001 and 2005. *Biogeosciences*, **9**, 3357–3380.

Masek JG, Collatz J (2006) Estimating forest carbon fluxes in a disturbed southeastern landscape: integration of remote sensing, forest inventory, and biogeochemical modeling. *Journal of Geophysical Research*, **11**, doi: 10.1029/2005JG000062, 2006

Meigs GW, Turner DP, Ritts WD *et al.* (2011) Landscape-scale simulation of heterogeneous fire effects on pyrogenic carbon emissions, Tree mortality, and net ecosystem production. *Ecosystems*, **14**, 758–775.

McCarty JL, Korontzi S, Justice CO, *et al.* (2009) The spatial and temporal distribution of crop residue burning in the contiguous United States. *Science of the Total Environment*, **407**, 5701–5712.

Moffat AM, Papale D, Reichstein M *et al.* (2007) Comprehensive comparison of gap-filling techniques for eddy covariance net carbon fluxes. *Agricultural and Forest Meteorology*, **147**, 209–232.

Moore DS, McCabe GP (2006) *Introduction to the Practice of Statistics* (5th edn). W.H. Freeman and Company, New York.

Myneni R, Hoffman R, Knyazikhin Y *et al.* (2002) Global products of vegetation leaf area and fraction absorbed PAR from one year of MODIS data. *Remote Sensing of Environment*, **76**, 139–155.

Nemani R, Hashimoto H, Votava P, *et al.* (2009) Monitoring and forecasting ecosystem dynamics using the Terrestrial Observation and Prediction System (TOPS). *Remote Sensing of Environment*, **113**, 1497–1509.

Olsen SC, Randerson JT (2004) Differences between surface and column atmospheric CO_2 and implications for carbon cycle research. *Journal of Geophysical Research-Atmospheres*, **109**, D02301.

Omernik JM (1987) Ecoregions of the conterminous United States. Map (scale 1:7,500,000). *Annals of the Association of American Geographers*, **77**, 118–125.

Pan Y, Chen JM, Birdsey R *et al.* (2011) Age structure and disturbance legacy of North American forests. *Biogeosciences*, **8**, 715–732.

Peters W, Jacobson AR, Sweeney C *et al.* (2007) An atmospheric perspective on North American carbon dioxide exchange: CarbonTracker. *Proceedings of the National Academy of Sciences of the United States of America*, **104**, 18925–18930.

Reichstein M, Ciais P, Papale D *et al.* (2007) Reduction of ecosystem productivity and respiration during the European summer 2003 climate anomaly: a joint flux tower, remote sensing and modelling analysis. *Global Change Biology*, **13**, 634–651.

Running SR, Baldocchi DD, Turner DP *et al.* (1999) A global terrestrial monitoring network integrating tower fluxes, flask sampling, ecosystem modeling and EOS satellite data. *Remote Sensing of Environment*, **70**, 108–128.

Schuh AE, Denning AS, Corbin KD *et al.* (2010) A regional high-resolution carbon flux inversion of North America for 2004. *Biogeosciences*, **7**, 1625–1644.

Schuh AE, Lauvaux T, West TO *et al.* (2013) Evaluating atmospheric CO_2 inversions at multiple scales over a highly inventoried agricultural landscape. *Global Change Biology*, **19**, 1424–1439.

Stephens BB, Gurney KR, Tans PP (2007) Weak northern and strong tropical land carbon uptake from vertical profiles of atmospheric CO_2. *Science*, **316**, 1732–1735.

Sun G, Caldwell P, Noormets A *et al.* (2011) Upscaling key ecosystem functions across the conterminous United States by a water-centric ecosystem model. *Journal of Geophysical Research-Biogeosciences*, **116**, G00J05.

Thomas CK, Law BE, Irvine J *et al.* (2009) Seasonal hydrology explains interannual and seasonal variation in carbon and water exchange in a semiarid mature ponderosa pine forest in central Oregon. *Journal of Geophysical Research-Biogeosciences*, **114**, G04006.

Thomas CK, Martin JG, Law BE *et al.* (2013) Toward biologically meaningful net carbon exchange estimates for tall, dense canopies: multi-level eddy covariance observations and canopy coupling regimes in a mature Douglas-fir forest in Oregon. *Agricultural and Forest Meteorology*, **173**, 14–27.

Turner DP, Cohen WB, Kennedy RE (2000) Alternative spatial resolutions and estimation of carbon flux over a managed forest landscape in Western Oregon. *Landscape Ecology*, **15**, 441–452.

Turner DP, Ritts WD, Cohen WB *et al.* (2005) Site-level evaluation of satellite-based global terrestrial gross primary production and net primary production monitoring. *Global Change Biology*, **11**, 666–684.

Turner DP, Ritts WD, Styles JM *et al.* (2006) A diagnostic carbon flux model to monitor the effects of disturbance and interannual variation in climate on regional NEP. *TellusB*, **58**, 476–490.

Turner DP, Ritts WD, Law BE, et al. (2007) Scaling net ecosystem production and net biome production over a heterogeneous region in the western United States. *Biogeosciences*, **4**, 597–612.

Turner DP, Ritts WD, Wharton S *et al.* (2009) Assessing FPAR source and parameter optimization scheme in application of a diagnostic carbon flux model. *Remote Sensing of Environment*, **113**, 1529–1539.

Turner DP, Göckede M, Law BE *et al.* (2011a) Multiple constraint analysis of regional land surface carbon flux. *TellusB*, **63**, 207–221.

Turner DP, Ritts WD, Yang ZQ *et al.* (2011b) Decadal trends in net ecosystem production and net ecosystem carbon balance for a regional socioecological system. *Forest Ecology and Management*, **262**, 1318–1325.

Turquety S, Logan JA, Jacob DJ *et al.* (2007) Inventory of boreal fire emissions for North America in 2004: importance of peat burning and pyroconvective injection. *Journal of Geophysical Research-Atmospheres*, **112**, D12S03.

Urbanski S, Barford C, Wofsy S *et al.* (2007) Factors controlling CO_2 exchange on timescales from hourly to decadal at Harvard Forest. *Journal of Geophysical Research-Biogeosciences*, **112**, G2.

USDA (2005) Crop Production, 2004 Summary. Available at: http://usda01.library.cornell.edu/usda/nass/CropProdSu//2000s/2005/CropProdSu-01-12-2005.pdf (accessed 25 March 2013).

Van der Werf GR, Randerson JT, Giglio L *et al.* (2006) Interannual variability in global biomass burning emissions from 1997 to 2004. *Atmospheric Chemistry and Physics*, **6**, 3423–3441.

Van Gorsel E, Delpierre N, Leuning R *et al.* (2009) Estimating nocturnal ecosystem respiration from the vertical turbulent flux and change in storage of CO_2. *Agricultural and Forest Meteorology*, **149**, 1919–1930.

Wallin MB, Grabs T, Buffam I *et al.* (2012) Evasion of CO_2 from streams — The dominant component of the carbon export through the aquatic conduit in a boreal landscape. *Global Change Biology*, **19**, 785–797.

Wang WL, Dungan J, Hashimoto H *et al.* (2010) Diagnosing and assessing uncertainties of terrestrial ecosystem models in a multimodel ensemble experiment: 1. Primary production. *Global Change Biology*, **17**, 1350–1366.

Welp LR, Randerson JT, Liu HP (2007) The sensitivity of carbon fluxes to spring warming and summer drought depends on plant functional type in boreal forest ecosystems. *Agricultural and Forest Meteorology*, **147**, 172–185.

Wharton S, Falk M, Bible K *et al.* (2012) Old-growth CO_2 flux measurements reveal high sensitivity to climate anomalies across seasonal, annual and decadal time scales. *Agricultural and Forest Meteorology*, **161**, 1–14.

Wilson KB, Baldocchi DD (2001) Comparing independent estimates of carbon dioxide exchange over 5 years at a deciduous forest in the southeastern United States. *Journal of Geophysical Research-Atmospheres*, **106**, 34167–34178.

Xiao XM, Zhang QY, Hollinger D *et al.* (2005) Modeling gross primary production of an evergreen needleleaf forest using MODIS and climate data. *Ecological Applications*, **15**, 954–969.

Xiao JF, Zhuang QL, Law BE *et al.* (2011) Assessing net ecosystem carbon exchange of U.S. terrestrial ecosystems by integrating eddy covariance flux measurements and satellite observations. *Agricultural and Forest Meteorology*, **151**, 60–69.

Xiao JF, Chen JQ, Davis KJ *et al.* (2012) Advances in upscaling of eddy covariance measurements of carbon and water fluxes. *Journal of Geophysical Research-Biogeosciences*, **117**, G00J01.

Yi CX, Ricciuto D, Li R *et al.* (2010) Climate control of terrestrial carbon exchange across biomes and continents. *Environmental Research Letters*, **5**, 034007.

Zhang L, Wylie BK, Ji L *et al.* (2011) Upscaling carbon fluxes over the Great Plains grasslands: sinks and sources. *Journal of Geophysical Research-Biogeosciences*, **116**, G00J03.

Zhang FM, Chen JM, Chen JQ *et al.* (2012) Evaluating spatial and temporal patterns of MODIS GPP over the conterminous US against flux measurements and a process model. *Remote Sensing of Environment*, **124**, 717–729.

Zhao MS, Heinsch FA, Nemani RR *et al.* (2005) Improvements of the MODIS terrestrial gross and net primary production global data set. *Remote Sensing of Environment*, **95**, 164–176.